CHAPTER VII

SURFACE ENHANCED RAMAN SCATTERING OF 1,4-DIMETHOXY-2-NITRO-3-METHYLANTHRANCENE-9,10-DIONE (DMNMAD) BY Ag NPs

Abstract

SERS has been employed to investigate the orientation of 1,4-dimethoxy-2-nitro-3-methylanthrance-9,10-dione(DMNMAD) molecule on Ag NPs. The Ag NPs were synthesized using a solution combustion method with citric acid as fuel. The nRs and SERS spectrum of DMNMAD molecule and DMNMAD molecule on Ag NPs have been simulated using DFT calculation at B3PW91 level of theory. The very good correlation found between experimental and theoretical data is a clear evidence for a reliable assignment of the vibrational bands. The large enhancement of C=O stretching and C-H in-plane modes in the SERS spectrum indicates that the molecules adsorbed on the Ag NPs may be adsorbed in a 'stand-on' orientation. The calculated HOMO and LUMO energy shows that charge transfer occurs within the molecule.

7.1 Introduction

Anthrodione (AD), also called as anthroquinone or dioxoanthracene, is an aromatic organic compound. It is the most important quinone derivative of anthracene [1]. Anthrodione derivatives have significant chemical and biochemical interest. They have various biochemical characteristics and have the wide application for medicines, pesticides, etc. [2]. These molecules have important applications as a prominent family of pharmaceutically active and biologically relevant chromophores, as an analytical tool for the determination of metals, and in many aspects of electrochemistry. They have many biological activities, such as anti infection, decreasing blood lipids content, anticancer activity, therapeutic agents, etc. They are used as a potent antitumor drug, owing to their ability to intercalate the DNA of tumour tissues [3]. Plants containing anthrodione have been used for millennia as dyestuffs and purgatives [4]. Anthracene derivatives have shown wide applications for the development of dye stuff materials, redox active and optical sensors [5]. These derivatives are of major importance in obtaining luminescent materials with potential applications as materials for lasers, paints, luminescent photo layers and light-emitting devices [6]. In this present work, SERS spectral analyses of DMNMAD molecule on Ag NPs were studied. HOMO and LUMO analysis of DMNMAD molecule and DMNMAD molecule on Ag NPs were also investigated.

7.2 Computational methods

In the present investigation, commercially available software package Gaussian 03 [7] is used to analyze and estimate the characteristics of optimized geometries, charge transfers, vibrational modes and the Raman spectra of DMNMAD molecule and that of DMNMAD molecule adsorbed on silver. The simulated spectrum is then compared with experimental observations. Computational study was carried out at the DFT level using B3PWY functional and LANL2DZ basis set. LANL2DZ basis set uses an effective core for all atoms and is a popular standard choice for the theoretical methods involving transition metals and organometallic complexes [8]. Silver cluster, Ag_3, identified to be stable and reactive has been considered in this study for the theoretical computations [9]. To identify the theoretical configuration on adsorption, computations were performed using identical functional and basis sets for multiple initial orientations. Irrespective of the initial geometry orientations, the adsorption geometry was identified to be the one with DMNMAD at a ‘stand-on, orientation with respect to the silver cluster and the most stable geometry is reported. Convergence of

all the calculations together with the absence of imaginary vibrational frequencies confirms the attainment of a local minimum on the potential energy surface [10-13]. Theoretical calculations generally overestimate the fundamental vibrational frequencies because of basis set deficiencies, anharmonicity and neglected part of electron correlation associated with the DFT functional employed in the theoretical calculations. To overcome this, a scaling factor DMNMAD molecule was uniformly applied to all the computed wavenumber.

7.3 Experimental

7.3.1 *Materials*

The details of the chemicals used are similar as discussed in chapter III and V. DMNMAD molecule was synthesized according to the literature [14].

7.3.2 Synthesis of Ag NPs by solution combustion method

Ag NPs used in this study were synthesized by solution combustion method as discussed in chapter II, III and V.

7.3.3 Characterization

The details of the instruments used are similar as described in chapter III.

7.4 Result and Discussion

7.4.1 HOMO-LUMO studies

The most important orbitals in a molecule are frontier molecular orbitals: HOMO and LUMO, which is the result of a significant degree of intermolecular charge transfer (ICT) from the end-capping electron-donor groups through π-conjugated path. The strong charge transfer interaction through π-conjugated bridge results in significant ground state donor-acceptor mixing and the appearance of a charge transfer band in the electronic absorption spectrum. These molecules interact with other species. The HOMO-LUMO molecular orbital gap helps to characterize the chemical reactivity; optical polarizability and chemical hardness-softness of a molecule [15-19]. Surfaces for the HOMO-LUMO molecular orbitals were drawn to understand the bonding scheme of the title compound. Figure 7.1 (a) and (b) shows the calculated HOMO-LUMO molecular orbitals for DMNMAD and DMNMAD molecule with Ag NPs at DFT/B3PWY. The calculated energy gap of DMNMAD molecule is 2.81eV at DFT/B3PWY (figure 7.1 (a)). The chemical stiffness and faintness of a molecule is a superior suggestion of the chemical stability of the molecule. The molecules that contain small energy gap are more polarizable because they require small energy for excitation. The HOMO and LUMO (Figure 7.1 (b)) of

DMNMAD molecule on Ag shows the intermolecular interactions in Ag component have occurred mostly in HOMO level. This result in significant excited state DMNMAD molecule on Ag NPs mixing and the appearance of charge transfer band in the electron adsorption spectrum. By comparing both cases, energy band gap between HOMO–LUMO of DMNMAD molecule on Ag NPs combination (1.17eV) is lower than that of donor molecule (2.81eV) which indicates to strong intermolecular interaction. Moreover, the lower HOMO and LUMO energy gap explains the eventual charge transfer interaction taking place within the molecule which is responsible for the chemical activity of the molecule.

7.4.2 SERS Studies

7.4.2.1 Vibrational assignments

Figure 7.2 the optimized structure of AD before and after adsorption on a three atom silver cluster (DMNMAD and DMNMAD -Ag). The nRs and SERS spectrum are shown in figures 7.3 and 7.4 respectively. Difference in the vibrational modes and Raman intensities of DMNMAD molecule and DMNMAD-Ag in theoretical and experimental spectra are analyzed to derive additional information on the nature of DMNMAD-Ag adsorption (table.7.1). Theoretical values of vibrational frequencies generally differ slightly from the experimentally observed frequencies because an isolated molecule in vacuum is considered for the theoretical calculations whereas the experimental results are of large molecules in each other's electrostatic environments in the solid state.

Generally, the carbonyl stretching vibration of various carbonyl groups occurs in the region 1810-1600cm^{-1}. The C=O stretching frequency is lowered appreciably when the substituent is capable of forming a hydrogen bond with the carbonyl group [20]. In the present case, the theoretical value of C=O stretching mode was observed in the region 1670-1581cm^{-1} in both nRs and SERS and experimental peak was observed at 1664-1582cm^{-1}in nRs and SERS band observed in the region 1684-1573cm^{-1} are assigned to C=O stretching of AD.

The aromatic ketones ring (C-C) stretching vibrations are very much important in the spectrum of athracene derivatives and are highly characteristic of the aromatic ring itself. AD, ring C-C stretching vibrations were observed in the region 1600-1250cm^{-1} [21]. In view of that, the C-C aromatic stretches were observed in region 1582-1273cm^{-1} in nRs spectrum and a strong peak were observed in region 1573-1267cm^{-1} in the SERS Spectrum. These vibrations are in good agreement with

the theoretical assignments were derived based DFT method. The C-C stretching vibration, which were assigned to coupled vibration of C-N, NO_2 modes and CH_3 deformation vibrations.

The C-H in plane bending vibrational modes usually occurs in the region 1300-1000cm^{-1} and is very useful for characterization purposes [22]. In the present case theoretical, nRs and SERS spectrum of C-H in-plane bending vibrational modes observed in the region 1340-985cm^{-1} are comparable with the experimental nRs peaks observed in the region 1324-986cm^{-1} and the strong–medium intensity of SERS peaks in the region 1327-995cm^{-1} are assigned to C-H in-plane bending vibration as reported in table.7.1. The aromativity of the compound was obviously proved by the presence of strong peak below 900cm^{-1} and substitution patterns on the ring can be judged from the out-of-plane bending of the ring C-H bond in the region 900-675cm^{-1} which is more informative [23]. In the present study, the theoretical values of C-H out-of-plane bending vibrational modes occur in the region 765-619cm^{-1} in both nRs and SERs. The experimental peaks were observed at 743-624cm^{-1} in nRs and the weak and medium bands of SERS occur in the region 903-626cm^{-1} confirm the C–H out of plane bending vibrations which agrees well with the above said literature values. In general the aromatic C–H vibratiional modes (in-plane and out-of-plane bending) are in good agreement with experimentally observed values [24]. The changes in the frequencies of these deformations from the values in anthracene are almost determined exclusively by the relative position of the substituent and are almost independent of their nature.

The characteristic group frequencies of the nitro group are relatively independent of the rest of the molecule which make this group convenient to identify. Aromatic nitro compounds have strong absorption due to the asymmetric and symmetric stretching vibrations of the NO_2 group in the range 1550-1490cm^{-1} and 1360-1320cm^{-1} respectively [24]. In the present case, the nRs band was observed in region 1545cm^{-1} and SERS bands occurring in the region 1552-1477cm^{-1} were assigned asymmetric NO_2 stretching vibrational mode and symmetric stretching of NO_2 vibrational mode occurred in the region 1372-1324cm^{-1} in both nRs and SERS and are in good agreement with the theoretical value.

For aromatic compounds, the C-N stretching vibration usually occurs in the region 1280-1180cm^{-1} [25]. In the present case, medium and weak vibrational mode occurring at 1273-1197cm^{-1} in nRs and at 1285-1186cm^{-1} in SERS are assigned to

C-N stretching vibrational mode. The ring breathing vibration mode is observed 1000cm^{-1} [26]. In the present case, ring breathing modes are observed in the region 986 and 995cm^{-1} in both nRs and SERS. The skeletal deformation vibrational mode occurs in the region 600-250cm^{-1} [27]. The observed nRs band around 536-258cm^{-1} and SERS band around 508-280cm^{-1} were assigned to skeletal deformation of title molecule (DMNMAD). These assignments are also in excellent agreement with the theoretical value.

The O-CH_3 mode is assigned to the region 1100-1000cm^{-1}[28, 29]. In present work, O-CH_3 stretching vibrational mode are identified in the region 1099-1031cm^{-1} in both nRs and SERS. The assignment of asymmetric and symmetric CH_3 deformation vibrations is more difficult as the spectra in the region are complex as several C-C stretching also appear in the same region [30] the assigned asymmetric and symmetric methyl deformations occur in the region 1488-1466cm^{-1} and 1380-1377cm^{-1}. The nRs and SERS band at 1456 and 1477cm^{-1} has been assigned to CH_3 asymmetric deformation mode in the present molecule. The observed nRs band at 1386cm^{-1} and SERS band around 1392-1372cm^{-1} were assigned to CH_3 deformation symmetric of title molecule (DMNMAD). The CH_3 torsion vibrational modes are observed at 152cm^{-1} in Raman spectrum and SERS vibrational mode is observed in the region 155cm^{-1}. The methyl group assignments proposed in this study is also in agreement with the literature values [31-33].The band at 226cm^{-1} is due to the stretching mode between metal and adsorbate. In most of the study on oxygen heterocycles adsorbed on silver electrodes, this line is recognized to the weak Ag-O bond [34, 35]. In the present case, the SERS band observed at 220$cm^{-1}$was assigned as Ag-O stretching vibrational mode are in good agreement with the theoretical values

7.4.2.2 Orientation of DMNMAD molecule and DMNMAD molecule on Ag NPs

The adsorption mechanism of an adsorbate can be deduced from its SERS spectrum. The possible potential sites available for the adsorption of title molecule on a Ag NPs are the anthrodionoe ring and carbonyl group. The orientation of the adsorbate on the metal nanoparticles will depend on these binding sites through which the interaction takes place. The possible orientation of the title molecule on the Ag NPs are lying down (flat-on) on the Ag NPs through bonding with the ring system or standing up (end-on). The orientation of the molecule on the Ag NPs can be inferred

from aromatic C-H stretching vibrations, ring stretching vibrations, the ring breathing mode, in-plane and out-of-plane vibration and SERS selection rule.

There are two enhancement mechanisms which generally describe SERS effect, the electromagnetic mechanism and the chemical mechanism. The enhancement in chemical mechanism is associated with an increase in the molecular polarizability of the adsorbate due to the charge transfer interaction of the adsorbate with the metal nanoparticles surface. In the electromagnetic mechanism, local electric fields in the surrounding of the metal nanoparticles were enhanced due to the surface plasmon excitation, leading to more intense electromagnetic transitions in molecules located near the nanoparticles, and enhanced Raman scattering. This can also be explained on the basis of the shift and the change in the relative intensities of the SERS bands when compared with the corresponding nRs spectrum.

The orientation of the adsorbed molecule is also inferred from the relative intensity of in-plane and out-of-plane modes. If the benzene ring is adsorbed flat on to the Ag NPs, its out-of-plane bending modes will be more enhanced when compared with its in-plane bending modes and if benzene ring is adsorbed 'stand-on' to the Ag NPs the in-plane bending modes will be more enhanced when compared with its out-of-plane bending modes vice-versa when adsorbed perpendicular to the surface [36].

The position of the ring breathing mode represents sufficient information of the orientation in the aromatic compound, title molecule. The ring breathing mode of SERS occurs at 995cm^{-1} and the bandwidth was decreased, compared to 986cm^{-1} for nRs. In the SERS spectra, the metal- molecule interaction increases the frequency of the ring breathing mode when compared to the spectrum of the free molecule in the solid state. It clearly suggests that title molecule is adsorbed on the Ag NPs in an 'end-on' orientation.

Commonly, quinone derivatives are adsorbed on the metal nanoparticles through the C=O binding site. The intensity of this peak increases and the wavenumber is downshifted with respect to the corresponding nRs bands [37]. In the present case, the carbonyl stretching vibration mode in SERS is upshifted, the bandwidth is increased and the intensity is reduced. The observed low intensity of this band may be due to the intermolecular hydrogen bond between the quinoid oxygen. The carbonyl oxygen makes an excellent binding site for surface adsorption

over the metal nanoparticles. When the carbonyl groups are binding to the metal nanoparticles, the wavenumber of the C=O stretching mode is increased [37]. The nRs and SERS shows four C=O stretching vibration modes that occur in the region 1684-1573cm^{-1}. The band at 1684cm^{-1} in SERS is upshifted in nRs spectrum and bandwidths are affected. Further, the vibrations of C=O stretching modes increases with respect to nRs. It was clearly proposed that DMNMAD molecule was adsorbed on the Ag NPs in a 'stand-on' orientation. In the present work, a new strong band appears at 220cm^{-1} in SERS was due to Ag-O stretching vibration [34, 35]. An intensity of Ag-O peak noticed at 211cm^{-1} and 220cm^{-1} in the theoretical and experimental spectra respectively of DMNMAD-Ag potentially confirms the process of adsorption as the pertain to the DMNMAD-Ag vibration and are absent in the case of DMNMAD. The important enhancement of Raman intensities is reminiscent of a strong adsorptions mechanism taking place between the DMNMAD molecule and Ag NPs.

Comparison of the relative intensities of the in-plane and out-of-plane modes shows that in-plane modes are more intense than out-of-plane modes. The presence of intense in-plane C-H bending modes in SERS suggests a strong adsorption interaction of AD on Ag NPs. Moreover, enhancement identified for out-of-plane C-H bending vibrational modes in the theoretical and experimental SERS imply a definite angle between the ring and the Ag NPs, further indicating a 'stand-on' orientation of the adsorbate on the surface [22-23]. The C-C stretching vibration modes are mainly important in the spectrum of AD and its derivatives are highly characteristic of aromatic ring. Medium intensity of bands generally occurs in the region 1600-1250cm^{-1} [21]. The ring modes are red shifted by around 10cm^{-1} along with increase in their bandwidth as the surface ring π orbital interaction is driving force of the surface adsorption. In the present case, the ring stretching band occurs in the region 1582-1267cm^{-1} in both nRs and SERS. The bands at 1552, 1423, 1392 and 1327cm^{-1} in SERS are upshifted in the nRs spectrum and their bandwidths are hardly affected. The enhancement in intensity of these vibrational mode mutually with the blue shifting of the ring stretching mode corroborate that the interactions between the ring and Ag NPs are very strong and confirm the 'stand-on' orientation of DMNMAD molecule on Ag NPs.

The enhancement skeletal deformation of AD, CH_3 torsion, symmetric and asymmetric NO_2 and O-CH_3 deformation more shore up the orientation of DMNMAD molecule on Ag NPs is ‘stand-on’ orientation of the benzene ring moiety on a Ag NPs. In conclusion, the result confirms that the orientation of DMNMAD molecule on an Ag NPs is ‘stand-on’.

7.5 Conclusion

Ag NPs were synthesized using solution combustion method with citric acid as fuel. nRs and SERS spectrum of DMNMAD and DMNMAD-Ag were assignment based on the DFT theoretically spectra. The very good correlation found between the experimental and theoretical data is a clear evidence for a reliable assignment of all vibrational bands. SERS is a good technique for studying the adsorption of molecule on Ag NPs. The nRs and SERS spectral analysis reveals that the DMNMAD molecule adsorbed ‘stand-on’ orientation on the Ag NPs. The HOMO-LUMO analysis confirms energy gap value has significant influence on the intermolecular charge transfer that the DMNMAD and DMNMAD-Ag has quite established configuration.

Reference

[1] J. Schripsema, V.A. Ramos, R. Verpoorte, Phytochem., 5 (1999) 55.

[2] L. Yanzhu, D. Min, S. Ziweri, T. Singhua, Sci. Technol., 4 (1999) 4.

[3] J.W. Lown, Chem. Soc. Rev., 1 (1993) 65.

[4] M. Hirsikorpi, T. Kamarainen, T. Teeri, A. Hohtola , Plant Sci., 162 (2002) 537.

[5] R.H. Thomson, Naturally occurring Quinones. Academic, NewYork, (1971).

[6] S. Khoee, S. Zamani, J. Eur. Polym., 43 (2007) 1272.

[7] L.S. Nair, C. T. Laurencin, J. Biomed. Nanotechnol., 3 (2007) 301.

[8] K.S. Lee, M.A. El-Sayed, J. Phys. Chem. B., 110 (2006) 19220.

[9] P. K. Jain, X. Huang, I.H. El Sayed, M.A. EL Sayed, Acc. Chem. Res., 41 (2008) 1578.

[10] N.C. Mueller, B. Nowack, Environ. Sci. Technol., 42 (2008) 4447.

[11] M. Fleishman, P.J. Hendra, A. McQuillan, Chem. Phys. Lett., 26 (1974) 163.

[12] A. Otto, J. Raman Spectrosc., 3 (2003) 593.

[13] J. Jiang, K. Bosnick, M. Maillard, L. Brus, J.Phys. Chem. B., 107 (2003) 9964.

[14] O.Khoumeri, M.Montana, T.Terme, P. Vanelle,.P, First, Tetrahedron., 64 (2008) 11237.

[15] J.R. Lombardi, R.L. Birke, Acc. Chem. Res., 42 (2009) 734.

[16] K. Kneipp, M.Moskovits, H. Kneipp, Surface Enhanced Raman Scattering, Springer: Berlin, (2006).

[17] J.A. Creighton, Surf. Sci., 124 (1983) 209.

[18] M. Moskovits, J.S. Suh, J. Phys. Chem., 88 (1984) 5526.

[19] S.K. Freeman, Application of Laser Raman Spectroscopy, Wiley, New York, (1974).

[20] B.S. Yadava, A. Israt, P. Kumar, P. Yadav, Indian J Pure & Appli phys., 43 (2003) 573.

[21] M. Pagannone, B. Formari, G. Mattel, Spectrochim, Acta A., 43 (1986) 621.

[22] J. Mohan, organic Spectroscopy Principle and Applications, 2nd ed., Narosa Publishing House, New Delhi. (2011) 30.

[23] V. Kirshnakumar, V. Balachandran, spectrochim Acta A., 61 (2005) 1001.

[24] B. Joseph Lambert, Introduction to Organic Spectroscopy., Macmillan Publications, New York, (1987).

[25] G. Joshi, N.L. Singh, Spectrochim. Acta A., 23 (1967) 1341

[26] N.P.G. Reoeges, A Guide to the Complete Interpretation of Infrared Spectra of Organic Structure, Wiley; New York, (1994).

[27] M.,Umadevi P. Vanelle, T. Terme, V. Ramakrishnan, J Raman Spectrosc., 34 (2003) 172.

[28] N.L. Owen, R.E. Hester, Spectrochim. Acta A., 25 (1969) 343.

[29] G.E. Campangnaro, J.L. Wood, J. Mol. Struct., 6 (1970) 117.

[30] E.F. Mooney, Spectrochim Acta A., 20 (1964) 1343.

[31] M. Karabacak, M. Cinar, S. Ermec, M. Kurt, J. Raman Spectrosc., 41 (2010) 98.

[32] A.U. Rani, N. Sundaraganesan, M. Kurt, M. Cinar, M. Karabacak, Spectrochim. Acta A., 75 (2010) 1523.

[33] C.Sengamalai, M.Arivazhagan, K.Sampathkumar, Elixir. Comp. Chem., 56 (2013) 13291.

[34] A.K Ojha, A. Singh, S. Dasgupta R. K. Singh, A. Roy, Chem. Phys. Letter., 431 (2006) 121.

[35] P.S. Mdluli, N.M. Sosibo, N. Revrapasadu, P. Karmanis, J. Leszczynski, J. Mol. struct., 935(2009) 32.

[36] J.S. Suh, M. Moscovits, J. Am. Chem. Soc., 108 (1986) 4711.

[37] G. Ramakrishna, P. Mohandas, S. Umapathy, J. Phys. Chem., 100 (1996) 16472.

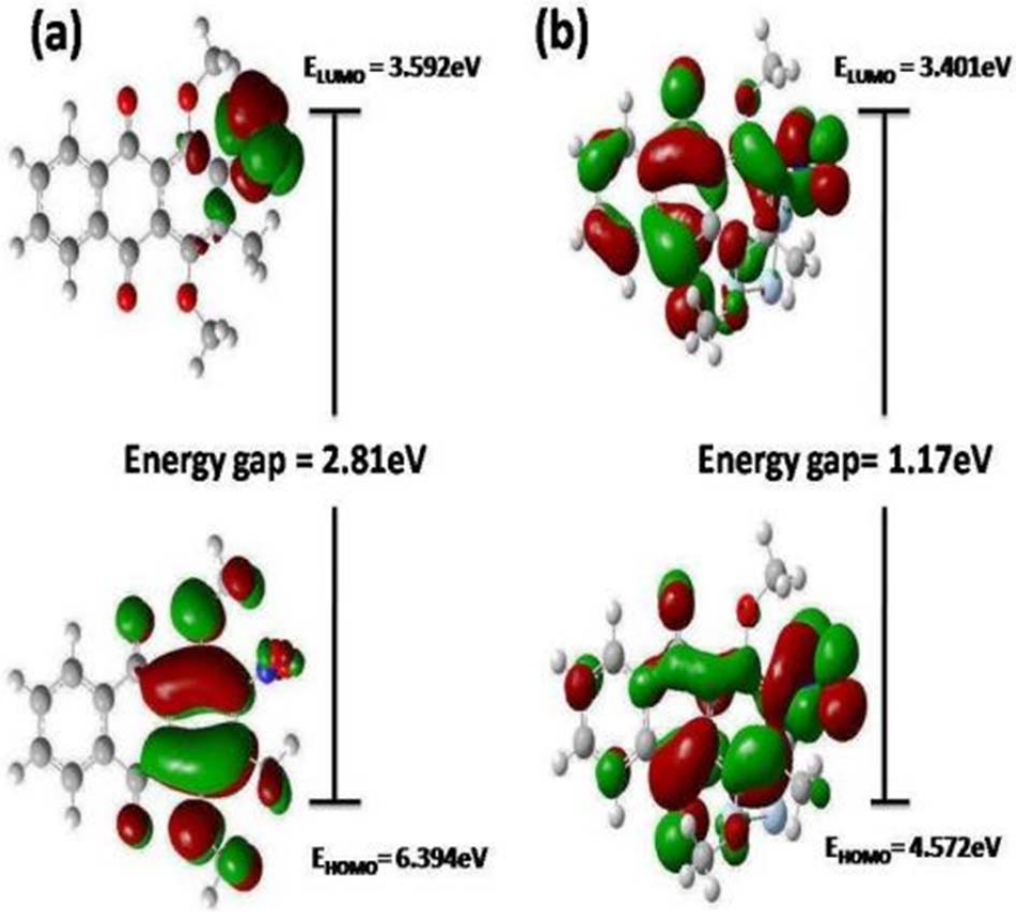

Figure 7.1 HOMO and LUMO plot of (a) DMNMAD molecule and (b) DMNMAD molecule on Ag NPs.

(a)

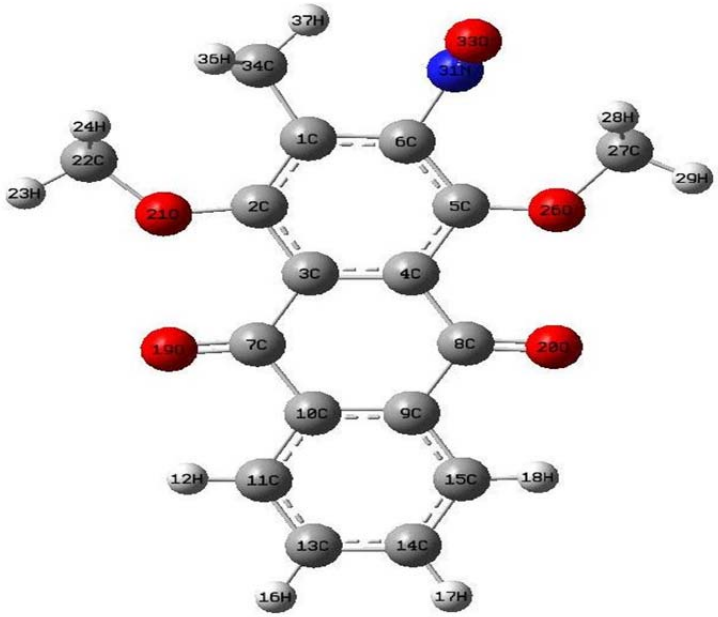

(b)

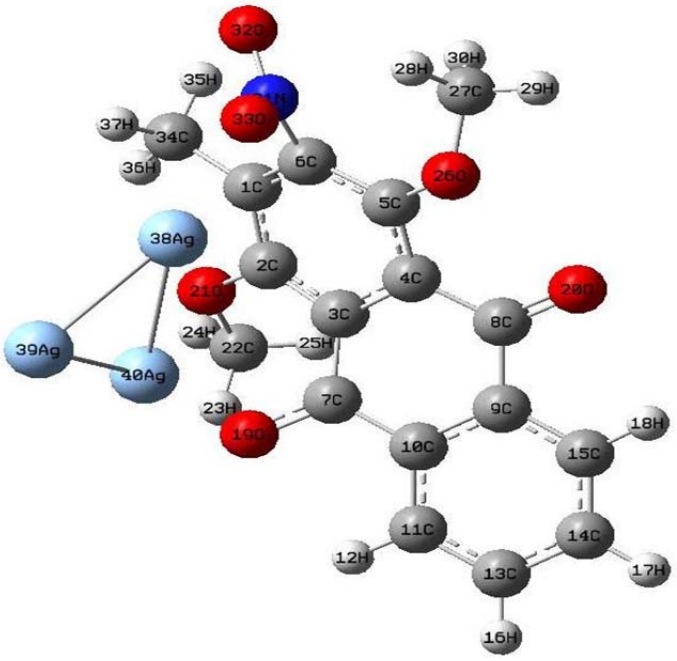

Figure 7.2 Optimized geometries of (a) 1,4-dimethoxy-2-nitro-3-methylanthrance-9,10-dion (DMNMAD) molecule and (b) DMNMAD molecule on Ag NPs.

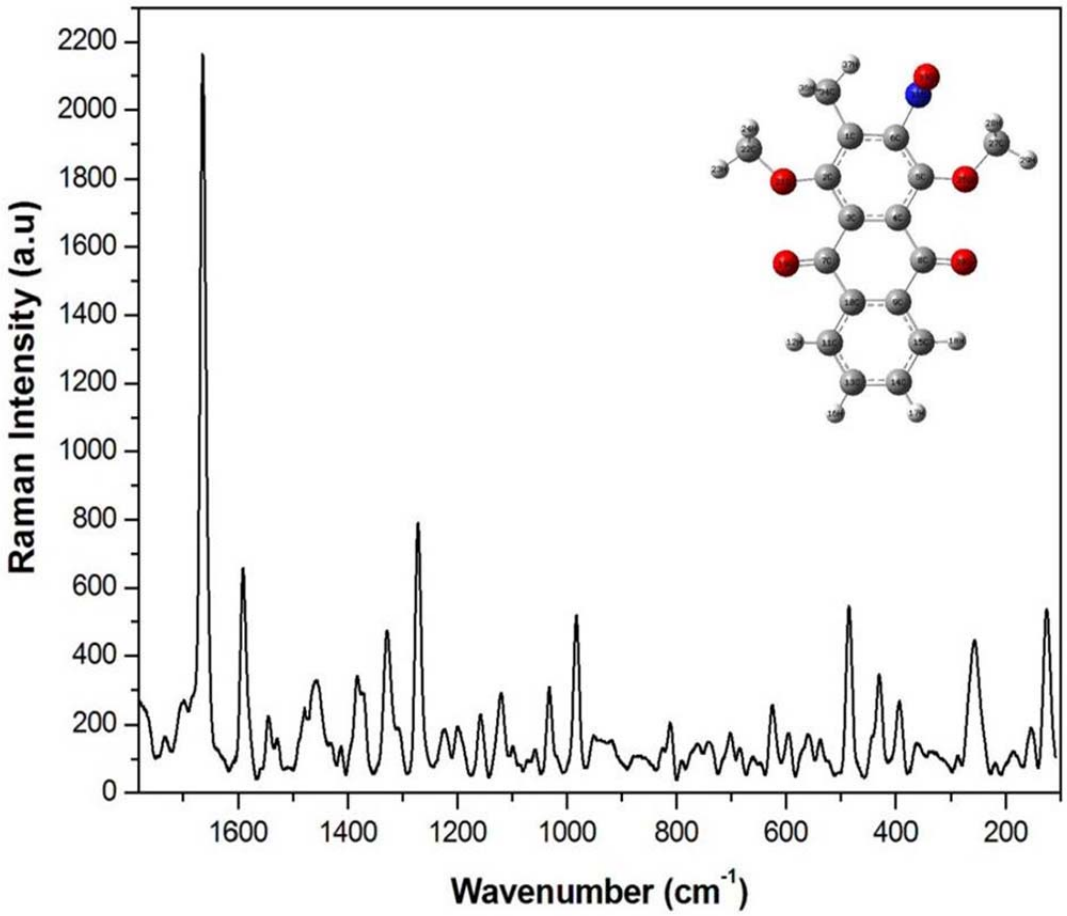

Figure 7.3 Normal Raman Spectrums (nRs) of DMNMAD molecule.

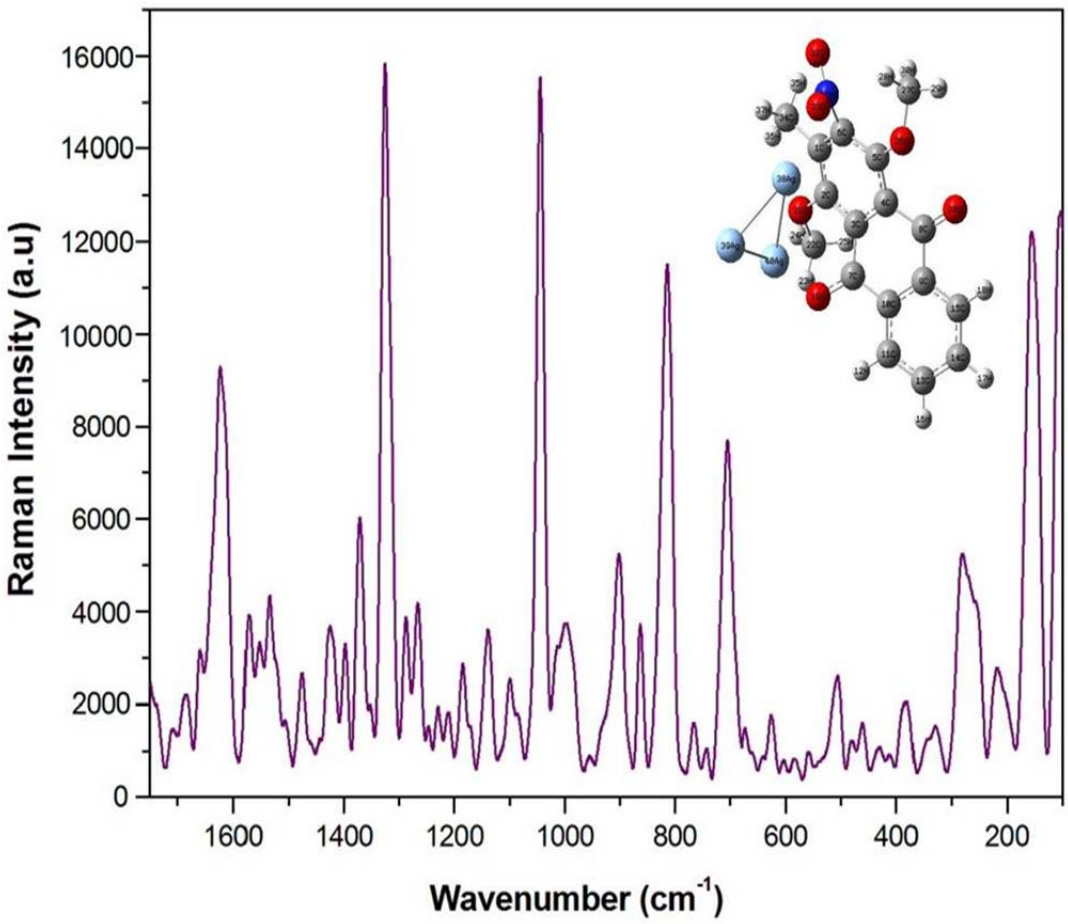

Figure 7.4 Surface Enhanced Raman Spectrums (SERS) of DMNMAD on Ag NPs.

Table 7.1 Vibrational assignment of DMNMAD molecule and DMNMAD molecule on Ag NPs.

nRs (cm^{-1})		SERS (cm^{-1})		Assignments
Theoretical	Experimental	Theoretical	Experimental	
1670	1664	1661	1684	C=O str.
		1615	1621	C=O str.
1596	1582	1581	1573	C=O str., C-C str.
1550	1545		1552	C-C str., asy. NO_2 str.
		1516	1535	C-C str., asy. NO_2 str.
		1497	1477	C-C str., asy. NO_2, asy. CH_3 def.
1440	1456			C-C str., asy. CH_3 def.
	1413		1423	C-C str.
1398	1386	1407	1392	sym. CH_3 def., C-C str.
			1372	sym. NO_2 str., sym. CH_3 def., C-C str.
1340	1324	1338	1327	C-H i.p., sym. NO_2 str., C-C str.
		1290	1285	C-H i.p., C-N str., C-C str.
1290	1273		1267	C-H i.p., C-N str., C-C str.
1233	1224		1228	C-H i.p., C-N str.
		1215	1210	C-H ip, C-N str.
	1197	1170	1186	C-H i.p., C-N str.
1160	1158			C-H i.p.
		1139	1143	C-H i.p.
	1120			C-H i.p.
			1099	C-H i.p., O-CH_3 str.
	1035	1030	1045	C-H i.p., O-CH_3 str.
1036	1031			C-H i.p., O-CH_3 str.
985	986	981	995	C-Hi.p., ring breathing

	931			C-H i.p.
			903	C-H o.p.
		850	865	C-H o.p.
			814	C-H o.p.
765	743	752	763	C-H o.p.
		716	706	C-H o.p.
619	624	645	626	C-H o.p.
520	536			skel. def. AD
		489	508	skel. def. AD
471	481			skel. def. AD
	393		403	skel. def. AD
		395	383	skel. def. AD
	359			skel. def. AD
			331	skel. def. AD
			280	skel. def. AD
	258			skel. def. AD
		211	220	Ag-O str.
	152	145	155	CH_3 tor.

str.- stretching, def.- deformation, i.p.-in-plane bending, o.p.-out-of-plane bending, rock.-rocking, skel.-skeletal, tor.-torsion, asy.-asymmetric, sy.-symmetric.